Search for Lepton Flavour Violation in the Decay $\tau^{\pm} \to \mu^{\pm}\gamma$

J. M. Roney

Department of Physics and Astronomy,
University of Victoria,
P.O.Box 3055 STN CSC,
Victoria, B.C., V8W 3P6, CANADA
(representing the BABAR Collaboration)

Abstract

A search for the lepton flavour violating decay $\tau^{\pm} \to \mu^{\pm}\gamma$ has been performed using $221.4\,\mathrm{fb}^{-1}$ of data collected at an e^+e^- centre-of-mass energy of 10.58 GeV with the BABAR detector at the PEP-II storage ring. The search has an efficiency of 7.45±0.65% for an expected background level of 6.2±0.5 events. In the final sample 4 candidate events are selected. As there is no evidence for a signal in this data, for this preliminary result we set an upper limit of $\mathcal{B}(\tau^{\pm} \to \mu^{\pm}\gamma) < 9 \times 10^{-8}$ at 90% CL using the method of Feldman and Cousins.

To be published in the Proceedings of the
8th International Workshop On Tau Lepton Physics
14-17 September 2004, Nara, Japan

Stanford Linear Accelerator Center, Stanford University,Stanford, CA 94309

Decays violating lepton flavour number, if observed, would be among the most theoretically clean signatures of new physics. The decay $\tau^\pm \to \mu^\pm\gamma$ is one such process and is expected with potentially observable rates in supersymmetric models[1–3], left-right supersymmetric models[4] and supersymmetric string unified models[5]. For some ranges of model parameters, decay rates as high as several parts per million are expected for this decay[3,5], even in light of the current experimental limit on the related $\mu^\pm \to e^\pm\gamma$ decay[6]. The recently reported non-zero charge-parity asymmetry in b-s radiative penguin processes[7] also suggests large $\mathcal{B}(\tau^\pm \to \mu^\pm\gamma)$ in grand unified theories with supersymmetry[8]. On the other hand, the modest extensions to the standard model (SM) incorporating neutrino oscillations predict a branching ratio many orders of magnitude below experimental accessibility ($\approx 10^{-40}$[9]). Therefore a discovery of this decay would require new physics and a non-observation of the decay would place restrictions on the parameters in the theories predicting large branching ratios. Currently the most stringent limit is $\mathcal{B}(\tau^\pm \to \mu^\pm\gamma) < 3.1 \times 10^{-7}$ at 90% confidence level (CL) from the BELLE experiment[10] using $86.3\,\mathrm{fb}^{-1}$ of e^+e^- annihilation data.

The search for $\tau^\pm \to \mu^\pm\gamma$ decays reported here uses data recorded by the *BABAR* detector at the PEP-II asymmetric-energy e^+e^- storage ring operated at the Stanford Linear Accelerator Center. The data sample consists of an integrated luminosity of $\mathcal{L} = 205.4\,\mathrm{fb}^{-1}$ recorded at a centre-of-mass energy ($\sqrt{s}$) of $10.58\,\mathrm{GeV}$ and $16.1\,\mathrm{fb}^{-1}$ recorded at $\sqrt{s} = 10.54\,\mathrm{GeV}$. With a cross section for $e^+e^- \to \tau^+\tau^-$ at the luminosity-weighted $\sqrt{s}$ of $\sigma_{\tau\tau} = (0.89 \pm 0.02)$ nb[11], this data sample contains 1.97×10^8 $e^+e^- \to \tau^+\tau^-$ events.

The *BABAR* detector is described in detail in Ref.[12]. Charged particles are reconstructed as tracks with a 5-layer silicon vertex tracker and a 40-layer drift chamber (DCH) inside a 1.5-T superconducting solenoidal magnet. An electromagnetic calorimeter (EMC) consisting of 6580 CsI(Tl) crystals is used to identify electrons and photons. A ring-imaging Cherenkov detector is used to identify charged hadrons. The flux return (IFR) of the solenoid, instrumented with resistive plate chambers, is used to identify muons.

The signature of the signal process is the presence of an isolated μ and γ having an invariant mass consistent with that of the τ ($1.777\,\mathrm{GeV}/c^2$ [13]), the energy of the μ and γ ($E_{\mu\gamma}$) equal to $\sqrt{s}/2$ in the event centre-of-mass (CM) frame, and the characteristics of the other particles in the event consistent with a SM τ decay. Such events are simulated with higher-order radiative corrections using KK2f [11] where one τ decays into $\mu\,\gamma$ with a flat phase space distribution[14], while the other τ decays according to measured rates[15] simulated with Tauola [16,17]. The detector response is simulated with GEANT4 [18]. The simulated events for signal as well as SM background processes[11,16,17,19,20] are then reconstructed in the same manner as data. The dominant backgrounds are from SM $e^+e^- \to \mu^+\mu^-$ (γ) and $e^+e^- \to \tau^+\tau^-$ (γ) events.

Events with two or four well reconstructed tracks and zero net charge are selected. The thrust, calculated with all observed charged and neutral particles, is required to lie between 0.9 and 0.975 to suppress $e^+e^- \to q\bar{q}$ background with low thrust and $e^+e^- \to \mu^+\mu^-$ and Bhabha backgrounds with thrust close to unity. In order to ensure the presence of at least one ν within the acceptance of the detector, the lab-frame polar angle (θ_{miss}) of the missing momentum of the event is required to lie within the geometrical acceptance of the detector ($-0.76 < \cos\theta_{miss} < 0.92$) and the missing CM transverse momentum (p^T_{miss}) is required to be significantly above zero: $-\ln(2 \times p^T_{miss}/\sqrt{s}) < 2(4)$ for events with two (four) tracks.

The signal-side hemisphere, defined with respect to the thrust axis, is required to contain one track with CM momentum less than $4.5\,\mathrm{GeV}/c$ and at least one γ with a CM energy greater than $200\,\mathrm{MeV}$. The track must be identified as a μ using DCH, EMC and IFR information and the γ candidate is the one which gives the mass of the μ γ system closest to the τ mass. The resolution of the mass of μ γ is improved by using a kinematic fit with $E_{\mu\gamma}$ constrained to $\sqrt{s}/2$ and by assigning the point of closest approach of the μ track from the e^+e^- collision axis to the origin of the γ candidate. This energy-constrained mass (m_{EC})

and $\Delta E = E_{\mu\gamma} - \sqrt{s}/2$ are independent variables in the absence of initial state radiation (ISR). The mean and width of the Gaussian core of the m_{EC} and ΔE distributions for reconstructed signal events are: $\langle m_{EC}\rangle = 1777\,\mathrm{MeV}/c^2$, $\sigma(m_{EC}) = 9\,\mathrm{MeV}/c^2$, $\langle\Delta E\rangle = $ -9 MeV, $\sigma(\Delta E) = 45\,\mathrm{MeV}$, where the shift in ΔE to low values comes from the tail induced by ISR.

Potential biases in the analysis are minimized by blinding the data events within a 3σ ellipse centred around $\langle m_{EC}\rangle$ and $\langle\Delta E\rangle$ in the m_{EC}-ΔE plane until all the optimization and systematic studies of the selection criteria have been completed.

In order to suppress $e^+e^- \to \mu^+\mu^-$ (γ) and $e^+e^- \to \tau^+\tau^-$ (γ) events containing energetic final state radiation and radiation in $\tau^\pm \to \mu^\pm\nu\bar{\nu}$ decays, an isolation criterion is imposed on the μ by requiring $|\cos\theta_H| < 0.8$, where θ_H is the angle between the μ momentum in the τ rest frame and the τ momentum as measured in the lab frame. Background contamination arising from $\tau \to h(\geq 1)\pi^0\nu$ decays with the hadronic track (h) mis-identified as a μ is reduced by requiring the sum of the CM energy of non-signal photon candidates in the signal-side to be less than 200 MeV. If the reconstructed neutral particle identified as the signal photon has at least a 1% likelihood of arising from overlapping daughters in $\pi^0 \to \gamma\gamma$ decays, the event is removed from consideration.

The tag-side hemisphere, which is expected to contain a SM τ decay, is required to have a total invariant mass less than $1.6\,\mathrm{GeV}/c^2$ and a CM momentum for each track less than $4.0\,\mathrm{GeV}/c$ to reduce background from $e^+e^- \to q\bar{q}$ and $e^+e^- \to \mu^+\mu^-$ processes, respectively. The $q\bar{q}$ background is further reduced by requiring the hemisphere to have no more than six photon candidates.

A tag-side hemisphere containing a single track is classified as e-tag, μ-tag or h-tag if the total photon CM energy in the hemisphere is no more than 200 MeV and the track is exclusively identified as an electron (e-tag), as a muon (μ-tag) or as neither (h-tag). If the total photon CM energy in the hemisphere is more than 200 MeV, then events are selected if the track is exclusively identified as an electron (eγ-tag) or as neither an

electron nor as a muon (hγ-tag). These allow for the presence of radiation in $\tau \to e\nu\bar{\nu}$ decays and for photons from $\pi^0 \to \gamma\gamma$ in $\tau \to h(\geq 1)\pi^0\nu$ decays. If the tag-side contains three tracks, the event is classified as a 3h-tag. We explored other tag-side channels but the sensitivity of the search does not improve by including them.

For the hadronic tagging modes, the invariant mass squared (m_ν^2) of the tag-side unobserved particle (assumed to be a ν_τ) can be well reconstructed assuming that the candidate $\tau^\pm \to \mu^\pm\gamma$ decay fully reconstructs the direction of τ in the tag-side with the energy of the τ given by $\sqrt{s}/2$. $|m_\nu^2|$ is required to be less than $0.4\,\mathrm{GeV}^2/c^4$ for h-tag and 3h-tag events and less then $0.8\,\mathrm{GeV}^2/c^4$ for hγ-tag events.

At this stage of the analysis 15% of the $\tau^\pm \to \mu^\pm\gamma$ signal events survive within a Grand Side Band (GSB) region defined as: $m_{EC} \in [1.5, 2.1]\,\mathrm{GeV}/c^2, \Delta E \in [-1.0, 0.5]\,\mathrm{GeV}$. In the non-blinded parts of the GSB, 4489 events survive in the data which agrees at the 5% level with the Monte Carlo (MC) background expectation of 4709 events. 80% of MC are $e^+e^- \to \tau^+\tau^-$ events, 82% of which are $\tau^\pm \to \mu^\pm\nu\bar{\nu}$ decays in the signal hemisphere.

To further suppress the backgrounds, separate neural net (NN) based discriminators are employed for each of the six tag-side channels. Five observables are used as input to the NN: the missing mass of the event, the CM momentum of the highest momentum tag-side track, $\cos\theta_H$, $-\ln(2 \times p_{miss}^T/\sqrt{s})$ and m_ν^2. Each NN is trained using data in the non-blinded part of the GSB to describe the background and $\mu\gamma$ MC in the full GSB region to describe the signal. The NN input distributions of the data are in good agreement with MC backgrounds both in shape and absolute rates as are the distributions of the NN outputs. The MC is then used to determine the cut values to be applied to the NN outputs by optimizing on the expected 90%CL upper limit[21] for observing a signal inside a 2σ ellipse in m_{EC}-ΔE plane centred around $\langle m_{EC}\rangle$ and $\langle\Delta E\rangle$.

The CM energy and momentum distributions of the γ and μ candidates before and after the NN selection has been applied are plotted in Figure 1. These distributions are also well described by the

Monte Carlo simulation in both shape and rates. The two dimensional plot of m_{EC} vs ΔE for data is shown in Figure 2 after the applying the NN selections.
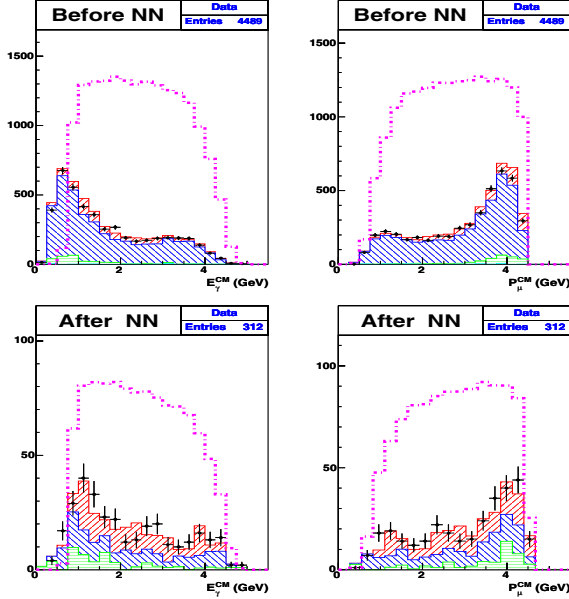

Figure 1. E_γ^{CM} and P_μ^{CM} in GSB Regions before and after the NN selection. Data are represented by points, background MC by hatched histograms ($e^+e^- \rightarrow \mu^+\mu^-$ is on top, $e^+e^- \rightarrow \tau^+\tau^-$ below it and $e^+e^- \rightarrow q\bar{q}$ on the bottom) and signal MC by dash-lined histograms.

The distributions for m_{EC} and ΔE before and after applying the NN selection are shown in Figure 3 where all channels have been combined. It is evident that there is good agreement between the data and MC in these observables. Because the missing mass is correlated with ΔE, after the NN selection is applied the remaining events tend to cluster towards low values of ΔE. Also shown in Figure 3 is the distribution of m_{EC} for events in $|\Delta E - \langle\Delta E\rangle| < 3\sigma(\Delta E)$ and the

distribution of ΔE when m_{EC} is restricted to $|m_{EC} - \langle m_{EC}\rangle| < 3\sigma(m_{EC})$.

The number of background events is estimated after all criteria are applied except that on m_{EC}. The estimate uses the non-blinded region inside the band in ΔE: $|\Delta E - \langle\Delta E\rangle| < 3\sigma(\Delta E)$, which we refer to as the m_{EC} sideband. As is evident from Figure 3 these events are fairly uniformly spread in m_{EC} and we estimate of the number of events in the blinded signal region by scaling the number of events in the sideband by the ratio of the area of the signal box to that of the sideband.
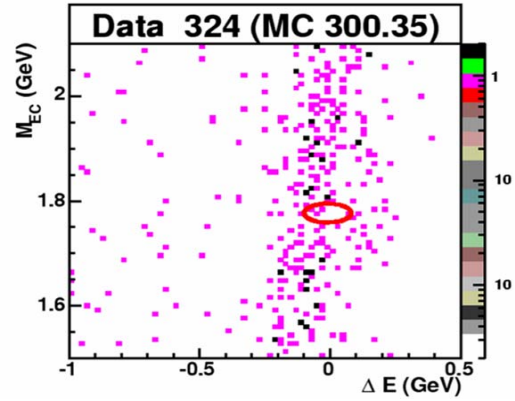

Figure 2. m_{EC} vs ΔE for data in all tag-side channels after applying the NN requirements. The number of events in the data and in the MC samples are quoted. The ellipse depicts the 2σ signal region.

For the MC in the 3σ blinded region, the background interpolation predicts 11.4 ± 0.9 events and 9.0 events are selected. This is to be compared with the data prediction of 14.0 ± 1.0 events
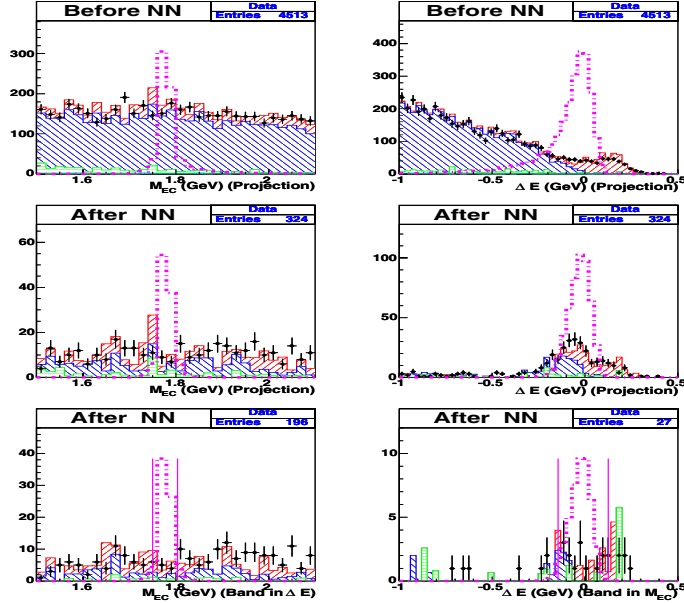
Figure 3. $m_{\rm EC}$ and ΔE in the full GSB Regions before and after the optimal NN requirement applied for all tag-side channels combined. Data are represented by points, background MC by hatched histograms, and signal MC by dash-lined histograms (with arbitary normalization). The selected number of events in the data is indicated in the upper right corner. The vertical lines indicate the 3σ binded region which is removed for the background estimation. In the lower left plot events lie within the band: $|\Delta E - \langle \Delta E \rangle| < 3\sigma(\Delta E)$ and in the lower right plot events lie within the band: $|m_{\rm EC} - \langle m_{\rm EC} \rangle| < 3\sigma(m_{\rm EC})$.

in this region. These 9.0 MC events correspond to 5.9 $e^+e^- \to \mu^+\mu^-$ events, 2.5 $e^+e^- \to \tau^+\tau^-$ events and 0.7 uds events. The $\tau^\pm \to \mu^\pm \nu \bar{\nu}$ decays account for four of the five $e^+e^- \to \tau^+\tau^-$ background events observed in the MC. The expectations for the number of background events in each tag-side channel are in good agreement with the number selected in the MC. Alternative means for estimating the background using the data yield consistent expected numbers of background events.

The numbers of events in data and MC in the GSB for the different tag-side channels are presented in Table 1 both before and after the NN selection. Also included in the table are the numbers of events in the MC that are selected in the 2σ signal region, the number of events in the sig-

nal region predicted from the MC sideband and the number of events predicted from the data sideband. There is reasonable agreement between the number of events observed in the data and those predicted by the MC for all tag-side channels both before and after the NN selection.

The relative systematic uncertainties on the trigger efficiency, tracking and photon reconstruction efficiencies, and particle identification are estimated to be 1.2%, 1.3%, 1.6% and 1.2%, respectively. We evaluate an uncertainty on the efficiency arising from the NN selection by fixing each NN input variable to its average value one at a time, without changing the architecture of the NN, and re-calculating the efficiency. This has the effect of removing each input variable completely from the NN selection procedure. This

results in 1.7% relative variation of the signal efficiency. Adding these errors in quadrature yields a combined systematic error estimate of 3.2%.

Alternatively, these (and other potential sources of systematic uncertainty not necessarily accounted for in the above procedure) can be collectively estimated from the uncertainty in the modelling of the detector by comparing data to the MC backgrounds in the non-blinded part of GSB, where the background and signal have similar properties apart from m_{EC} and ΔE. The statistical precision of this data-to-MC ratio is augmented by using an expanded m_{EC} range $\in [1.0, 2.5]\,\mathrm{GeV}/c^2$, where one selects 747 and 713 events in data and MC backgrounds, respectively. The error on this ratio $1.048\pm0.055(stat)\pm0.023(norm)$ is ascribed to the systematic error on efficiency, where the 2.3% normalization error arises from the error on the product $\mathcal{L}\sigma_{\tau\tau}$.

The tracking and calorimetry systematic errors affect primarily the uncertainties introduced by applying the final signal region requirement. These systematic effects are studied using a control sample of $e^+e^- \to \mu^+\mu^-$ events with energetic photons. In order to assess uncertainty on the efficiency arising from the mass and energy scale and resolution systematic errors, the ΔE and m_{EC} peaks were varied by $\pm4\,\mathrm{MeV}$ and their resolution by $\pm1\,\mathrm{MeV}$. Adding the deviations induced by these variations in quadrature yields an uncertainty of 6.3% on the efficiency. In addition, we estimate the uncertainty on the efficiency associated with the bean energy systematic error to be 0.6%. The total systematic uncertainty on the efficiency is 8.7%.

This analysis has an efficiency of $(7.45\pm0.65)\%$ and an expected background, determined from data estimates of the number of background events in the 2σ signal ellispe, N_{bkg}, of 6.2 ± 0.5. After unblinding we find 12 events in the blinded region (to be compared with 14.0 ± 1.0 expected) and 4 events in the signal region of our data sample. The probability of 6.2 fluctuating down to 4 events or fewer is 26 %. Table 1 lists how these 4 events are distributed across the different tag channels. There is good agreement between the observations and expectations in all tag channels in the unblinded and signal regions.

We calculate the branching fraction of the $\tau^\pm \to \mu^\pm\gamma$ decay based on a likelihood function, which convolutes a Poisson distribution with two Gaussian resolution functions for the background and the efficiency:

$$\mathcal{L}(n, \hat{b}, \hat{f}; B, b, f) = \frac{\mu^n e^{-\mu}}{n!} \frac{1}{2\pi\sigma_b\sigma_f} e^{-\frac{1}{2}\left(\frac{\hat{b}-b}{\sigma_b}\right)^2 - \frac{1}{2}\left(\frac{\hat{f}-f}{\sigma_f}\right)^2}$$

(1)

where B denotes the branching fraction of ($\tau^\pm \to \mu^\pm\gamma$), $f = 2N_{\tau\tau}\epsilon$, b is the expected total background, $\mu = \langle n \rangle = fB + b$, n is the number of observed events, and $\hat{b}$ ($\hat{f}$) is sampled from a normal distribution $N(b, \sigma_b)$ ($N(f, \sigma_f)$). The number of tau pair events $N_{\tau\tau}$ is 1.97×10^8. The errors on the efficiency and normalization are incorporated in σ_f. This yields a branching fraction of $\mathcal{B}(\tau^\pm \to \mu^\pm\gamma) = (-7.5^{+8.1}_{-6.2}) \times 10^{-8}$.

Since we have no evidence for a signal we have computed an upper limit. Using the method of Feldman and Cousins[21] the upper limit is 9×10^{-8} at 90%CL. The systematic errors do not change the limit for the number of significant figures quoted. *

This preliminary result reduces by more than a factor of three the current upper limit on the lepton flavour violating decay $\tau^\pm \to \mu^\pm\gamma$ established by the BELLE Collaboration.

REFERENCES

1. R. Barbieri and L. J. Hall, Phys. Lett. B **338**, 212 (1994)
2. J. Hisano, T. Moroi, K. Tobe, M. Yamaguchi and T. Yanagida, Phys. Lett. B **357**, 579 (1995)
3. J. Hisano and D. Nomura, Phys. Rev. D **59**, 116005 (1999)
4. K. S. Babu, B. Dutta and R. N. Mohapatra, Phys. Lett. B **458**, 93 (1999)
5. S. F. King and M. Oliveira, Phys. Rev. D **60**, 035003 (1999)
6. M. L. Brooks *et al.* [MEGA Collaboration], Phys. Rev. Lett. **83**, 1521 (1999) This work currently provides the most strin-

---

*Following a Bayesian approach, the upper limit using a uniform prior in the branching fraction, the background, and efficiency is $\mathcal{B}(\tau^\pm \to \mu^\pm\gamma) < 14 \times 10^{-8}$ at 90% CL.

Table 1
Tag-side dependence of the efficiency and no. events in the GSB, 3σ blinded region and 2σ signal region.

tag	$\mu\gamma$ Eff(%)	MC Backgrounds Grand Side-Band		MC Backgrounds Signal Region		Data Grand Side-Band		Data 3σ blinded Region		Data Signal Region	
		Before NN	After NN	Predict	Select	Before NN	After NN	Predict	Select	Predict	Select
e	1.27	889.7	44.7	0.7±0.2	0.0	889	52	2.3±0.4	3	1.0±0.2	1
eγ	0.18	142.4	2.7	0.0±0.0	0.0	140	6	0.2±0.1	0	0.1±0.1	0
m	1.31	1486.2	59.3	1.7±0.2	1.1	1379	63	4.3±0.6	2	1.9±0.3	1
h	0.89	303.5	18.1	0.4±0.1	0.0	318	29	1.1±0.3	1	0.5±0.1	0
hγ	2.57	1221.9	104.3	1.7±0.2	1.7	1160	88	4.1±0.6	5	1.8±0.3	1
3h	1.22	665.4	62.2	0.6±0.1	0.0	603	74	2.1±0.4	1	0.9±0.3	1
all tags	7.45	4709.1	291.3	5.1±0.4	2.8	4489	312	14.0±1.0	12	6.2±0.5	4

gent limit of $\mathcal{B}(\mu^{\pm} \to e^{\pm}\gamma) < 1.2 \times 10^{-11}$ at 90%CL.

7. B. Aubert *et al.* [BABAR Collaboration], arXiv:hep-ex/0408127. K. Abe *et al.* [BELLE Collaboration], arXiv:hep-ex/0408104.

8. Junji Hisano, Proceedings of 8th International Workshop on Tau-Lepton Physics, Nara, Japan September 14-17, 2004.

9. X. Y. Pham, Eur. Phys. J. C **8**, 513 (1999)

10. K. Abe *et al.* [Belle Collaboration], Phys. Rev. Lett. **92**, 171802 (2004)

11. B. F. Ward, S. Jadach, and Z. Was, Nucl. Phys. Proc. Suppl. **116**, 73 (2003).

12. *BABAR* Collaboration, B. Aubert *et al.*, Nucl. Instr. Meth. A **479**, 1 (2002).

13. BES Collaboration, J. Z. Bai *et al.*, Phys. Rev. D **53**, 20 (1996).

14. Although the signal MC has been modelled using a flat phase space model, the limit obtained in this analysis is insensitive to this assumption as demonstrated by considering the two extreme cases of a V-A and a V+A form of interaction for the signal MC.

15. Particle Data Group, K. Hagiwara *et al.*, Phys. Rev. D **66**, 010001 (2002).

16. S. Jadach, Z. Was, R. Decker, and J. H. Kuhn, Comput. Phys. Commun. **76**, 361 (1993).

17. E. Barberio and Z. Was, Comput. Phys. Commun. **79**, 291 (1994).

18. GEANT4 Collaboration, S. Agostinelli *et al.*, Nucl. Instr. Meth. A **506**, 250 (2003).

19. D. J. Lange, Nucl. Instrum. Meth. A **462**, 152 (2001).

20. T. Sjostrand, arXiv:hep-ph/9508391.

21. G. J. Feldman and R. D. Cousins, Phys. Rev. D **57**, 3873 (1998)